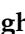




Article

An Online Estimation Method for the Equivalent Inertia Time Constant of Power Equipment Based on Node Power Flow Equations

Zhenghui Zhao ^{1,*}, Xianan Wang ¹, Jinhui Sun ¹, Yubo Sun ², Qian Zhang ³ and Yang Wang ¹

¹ School of Electrical Information Engineering, Jiangsu University, Zhenjiang 212013, China; 2222207119@stmail.ujs.edu.cn (X.W.); 2222407089@stmail.ujs.edu.cn (J.S.); wangjust@ujs.edu.cn (Y.W.)

² Department of Electrical Engineering, Tsinghua University, Beijing 100190, China; sunyb16@mails.tsinghua.edu.cn

³ School of Agricultural Engineering, Jiangsu University, Zhenjiang 212013, China; zhangq_jsu@ujs.edu.cn

* Correspondence: zhzhao@ujs.edu.cn

Abstract: As renewable energy integration scales up, power systems increasingly depend on sources interfaced through power electronic converters, which lack rotating mass and substantially diminish system inertia. This reduction in inertia, coupled with the complex and diverse control strategies governing power electronics, presents significant challenges in accurately assessing the equivalent inertia levels within modern power systems. This paper introduces an online method for estimating the inertia time constant of power nodes, grounded in the node power flow equation, to address these challenges. The approach begins by deriving the rotor motion equation for synchronous generators and defining the inertia time constant of power nodes through an analysis of the power flow equations. Real-time frequency and voltage phasor data are collected from system nodes using phasor measurement units. The frequency state of the power equipment is then characterized using a divider formula, and the equivalent reactance between the power equipment and the node is further derived through the node power flow equation. This enables the real-time estimation of the equivalent inertia time constant for power nodes within the system. The effectiveness of the proposed method is demonstrated through simulations on the WSCC9 system, confirming its applicability for real-time system analysis.

Keywords: inertia evaluation; inertial response; phasor measurement unit; online analysis; frequency stability



Citation: Zhao, Z.; Wang, X.; Sun, J.; Sun, Y.; Zhang, Q.; Wang, Y. An Online Estimation Method for the Equivalent Inertia Time Constant of Power Equipment Based on Node Power Flow Equations. *Energies* **2024**, *17*, 6214. <https://doi.org/10.3390/en17246214>

Academic Editor: Antonio T. Alexandridis

Received: 7 November 2024

Revised: 30 November 2024

Accepted: 5 December 2024

Published: 10 December 2024



Copyright: © 2024 by the authors. Licensee MDPI, Basel, Switzerland. This article is an open access article distributed under the terms and conditions of the Creative Commons Attribution (CC BY) license (<https://creativecommons.org/licenses/by/4.0/>).

1. Introduction

As fossil fuel resources are progressively exhausted and renewable energy technologies advance at a rapid pace, the integration of renewable energy into power systems has consistently grown, resulting in a gradual substitution of synchronous generators with non-synchronous sources [1,2]. The evolution of inertia resources in power systems is illustrated in Figure 1. However, incorporating these sustainable energy sources into the grid requires the extensive use of electronic conversion technologies, which effectively decouples them from the system's frequency. As a result, under traditional control methods, these units are unable to provide the required inertia support to the grid [3,4], thereby causing a substantial decrease in the overall inertia. During large disturbances, the rate of change of frequency (RoCoF) increases sharply compared to traditional power systems, heightening the risk of under-frequency load-shedding events in renewable units and increasing the likelihood of cascading failures, thereby posing a substantial risk to system frequency stability [5–7]. Assessing the inertia levels of grid-connected renewable units is thus essential for managing and supplementing inertia resources effectively, helping to address potential stability challenges associated with low inertia levels.

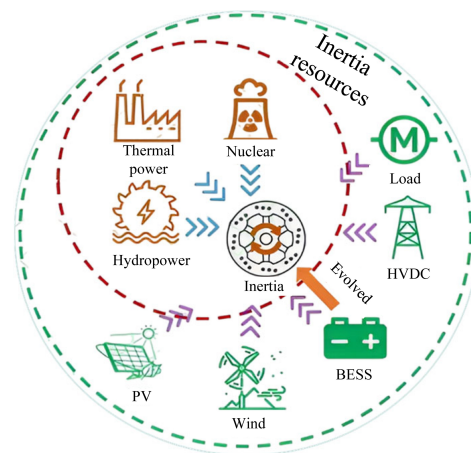


Figure 1. Evolution of power system inertia resources.

The proliferation of innovative energy devices has sparked a growing interest in assessing power system inertia, with a particular focus on online assessment methods. These methods provide critical insights for the scheduling and operation of power grids, enhancing their resilience to active power deficits and reducing the risk of unintended disconnection of new energy devices during low-frequency events. Such advancements ensure the continued integration of these devices into frequency regulation strategies. Extensive research has been conducted in this domain. For instance, references [8,9] employed sliding window processing techniques to analyze data captured by phasor measurement units (PMUs). By selecting an appropriate window length and sliding step size, they utilize the system's equivalent rotor motion equation to enable the estimation of inertia in real time. Additionally, wide-area measurement data, as described in [10], are leveraged to develop aggregated equivalent models based on frequency response characteristics. Techniques such as least squares, Newton-Raphson, and modal confidence criteria are then employed to efficiently identify system parameters, facilitating the determination of equivalent inertia. An alternative method, as outlined in reference [11], involves discretizing the system's equivalent rotor motion equation and selecting an appropriate time interval based on the power angle and active power at the generator bus, thereby enabling the determination of the system's equivalent inertia. In reference [12], a Markov switching model is constructed based on the correlation between the system's equivalent inertia and frequency fluctuations. Historical data is utilized to train and refine the model, enabling real-time evaluation of the system's equivalent inertia using PMU frequency measurement data under quasi-steady state conditions. It is important to highlight that the accuracy of this evaluation process depends on the availability of a substantial amount of historical measurement data, and it may face limitations in scenarios where data are scarce. Additionally, reference [13] introduces an inertia identification approach utilizing the energy function of synchronous generators and the concept of the generator port energy function. In this approach, the inertia identification window is optimized through linear fitting of the frequency response at the generator's outlet following a disturbance, which improves the accuracy of the inertia estimation. Reference [14] presents a novel method for adaptive predictive frequency control in multi-area power systems, specifically designed to handle unknown and time-varying inertia. However, the accuracy of this approach depends critically on the precise calculation of energy variations during power adjustments. Lastly, reference [15] focuses on regional power grids, utilizing sectional contact power and intra-regional load disturbances as inputs and frequency disturbances as the output. By employing an output error model, continuous estimation of regional inertia and the overall network's equivalent inertia is enabled during typical operating scenarios. The aforementioned methodologies collectively gather and analyze data from diverse perspectives, ultimately facilitating the estimation of power system inertia.

In summary, substantial research has been undertaken on the prediction and assessment of inertia levels within power systems. However, certain limitations still require attention:

- (1) Existing offline evaluation methods that rely on large disturbance events possess a constrained scope of application, and they can solely be used for post-accident system analysis, with a limited contribution to the optimal operation of the system. They also fall short when it comes to achieving real-time monitoring of the inertia state within the power system.
- (2) The current online inertia estimation approaches do not adequately account for the effects of the operational characteristics of different virtual inertia resources and their various uncertainties on the precision of system inertia evaluation. This can result in issues like poor robustness, reduced accuracy, and high computational load. Consequently, it is necessary to explore further the new online estimation methods of inertia that are applicable to normal operating conditions.

Inspired by the challenges outlined above, this paper introduces a real-time estimation approach for determining the inertia time constant of power equipment grounded in node power flow equations. Unlike offline analysis, which provides retrospective data due to inherent time lags, online analysis offers real-time insights, capturing dynamic changes in the system. As such, it places greater demands on computational speed. Our approach leverages power flow equations to evaluate the inertia time constant of power source nodes, relying solely on frequency and voltage phasor measurements from PMUs. This method is computationally efficient with low complexity, making it well-suited for the real-time analysis required in power systems. Importantly, the approach is derived from the rotor dynamics equation of synchronous generators, ensuring high accuracy in inertia time evaluation. The key contributions of this work are as follows:

- (1) The rotor motion equation for the synchronous machine is derived, and the inertia constant is defined to enable continuous calculation of the equivalent inertia time constant for any power generation unit.
- (2) By deriving from the node power flow equation, the variation of power and the incremental rate of frequency needed to calculate the equivalent inertia constant of power equipment are obtained.
- (3) The proposed method requires only real-time operational data from the node connected to the generation unit, collected via PMU devices, to estimate the equivalent inertia time constant. This approach is broadly applicable, offers fast computational speed, and demonstrates practical value for real-world implementation.

Simulations were conducted using Simulink software to assess the feasibility of the proposed approach. The results from these simulations highlight the capability of the approach in accurately determining the inertia characteristics of power generation units. The findings offer strong evidence supporting the approach's viability and reliability.

The remainder of this paper is organized as follows. In Section 2, the derivation of the estimation formula for the equivalent inertia time constant of power generation equipment is presented, and the unknown variables in the estimation formula are solved using the node power flow equation. Section 3 discusses a case study of the proposed estimation method applied to the WSCC 9-bus system, verifying the effectiveness, accuracy, and generality of the online estimation approach. Finally, Section 4 provides a conclusion and outlines directions for future work.

2. Online Estimation Method for the Equivalent Inertia Time Constant of Power Equipment

This paper presents a unified framework to assess the equivalent inertia across diverse power equipment by first deriving the inertia time constant for synchronous generators through a detailed analysis of the rotor motion equation. This concept is then extended to define the equivalent inertia time constant for power source nodes within the broader power system. Key variables are adjusted to ensure alignment with data captured by phasor measurement units (PMUs), facilitating the formulation of an equation to estimate

the equivalent inertia time constant of these nodes. An improved solution method is proposed to enhance solution accuracy and mitigate singularities caused by sign changes. The structure and components of Section 2 are illustrated in Figure 2.

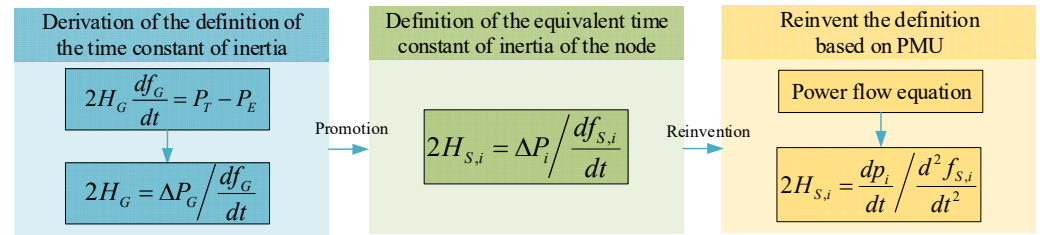


Figure 2. The specific components of Section 2.

In the event of a disturbance in the power system, the frequency response can be divided into three distinct stages: the inertial response, the primary response, and the secondary response. The initial inertial response, characterized by its brief duration, occurs when the input power of the prime mover temporarily exceeds its rated value. During this phase, the rotational inertia of the synchronous generator resists changes in the prime mover's speed, thereby slowing the rate of frequency variation in the power system. In this study, the equation of motion governing the synchronous generator rotor is analyzed, and the equivalent inertia time expression for nodes connected to power equipment is derived step by step.

This paper starts with a derivation based on fundamental equations. Equation (1) represents the rotor motion equation of a synchronous machine, with the effects of damping assumed to be negligible. It defines the connection between the synchronous generator's rotational inertia and the frequency. The input power from the prime mover [16,17]:

$$2H_G \frac{df_G}{dt} = P_T - P_E \quad (1)$$

where H_G represents the time constant of the synchronous generator's rotational inertia; f_G represents the actual operating frequency of the synchronous generator; P_T and P_E represent the mechanical power of the prime mover and the electromagnetic power, respectively.

Under normal operating conditions, the power system frequency remains stable, with the electromagnetic power output P_E of the synchronous generator balanced by the mechanical power input P_T from the prime mover, resulting in both sides of equation (1) being equal. At the moment a disturbance occurs, system frequency begins to fluctuate that $\frac{df_G}{dt} \neq 0$. The prime mover maintains its pre-disturbance input that $P_T^{0+} = P_T^0$, while the electromagnetic power output of the synchronous generator changes abruptly. At this point, the difference on the right side of Equation (1) corresponds to the magnitude of the disturbance, allowing Equation (1) to be rewritten as Equation (2):

$$2H_G = \Delta P_G / \frac{df_G}{dt} \quad (2)$$

where ΔP_G represents the active power deficit allocated to the synchronous generator after the power system experiences a disturbance.

Equation (2) serves as the definition for H_G . This paper extends this to derive the expression for the inertia time constant $H_{S,i}$ of the source S , connected to the system node i , as presented in Equation (3):

$$2H_{S,i} = \Delta P_i / \frac{df_{S,i}}{dt} \quad (3)$$

where $H_{S,i}$ represents the inertia time constant of the source S connected to the system node i ; ΔP_i represents the real power deficit of the node i allocated to the generation unit after

the power system experiences a disturbance; $f_{S,i}$ represents the actual operating frequency of the generation unit connected to the system node i .

In conclusion, the inertia time constant of a power node can be determined by measuring P_S and $f_{S,i}$. The active power P_S at power node s in the power system is represented by Equation (4):

$$P_i = U_i \sum_{j=1}^n U_j (G_{ij} \cos \theta_{ij} + B_{ij} \sin \theta_{ij}) \quad (4)$$

where U_i and U_j represent the voltage magnitudes at nodes i and j ; G_{ij} and B_{ij} represent the mutual conductance and mutual susceptance between nodes i and j , respectively; θ_{ij} represents the voltage phase angle difference between nodes i and j .

The voltage phasor and frequency at system nodes can be measured using PMU devices, enabling the calculation of active power at node i at any given time using Equation (4). However, it is not possible to directly determine the active power deficit ΔP_i at the node after a disturbance. Typically, the voltage magnitude U_i at the power node i remains constant, and G_{ij} can be assumed to be zero. As a result, Equation (4) can be expressed as a function of U_j and θ_{ij} . By differentiating both sides of Equation (4) with respect to time t , Equation (5) is obtained:

$$dp_i = \sum_{j=1}^n \frac{\partial p_i}{\partial \theta_{ij}} d\theta_{ij} + \sum_{j=1}^n \frac{\partial p_i}{\partial u_j} du_j \quad (5)$$

In summary, this paper derives the expression for dp_i , with all relevant parameters accessible through PMU devices. To align with this, by differentiating both sides of Equation (1) with respect to time t and making minor adjustments, a new definition for $H_{S,i}$ is obtained, as shown in Equation (6):

$$2H_{S,i} = \frac{dp_i}{dt} / \frac{d^2 f_{S,i}}{dt^2} \quad (6)$$

The parameter $f_{S,i}$ in Equation (6) can be determined using the divider formula [18], and its expression is given in Equation (7):

$$f_{S,i} = \Delta f_i - x_{S,i} \sum_{j=1}^n \frac{\partial p_i}{\partial \theta_{ij}} \frac{d\theta_{ij}}{dt} \quad (7)$$

where Δf_i is the deviation from the rated frequency on the node i . $x_{S,i}$ is the equivalent reactance between the power unit S and the node i .

The nodal power flow equations are employed to compute $x_{S,i}$. Since reactance is essential for the distribution of reactive power in power flow analysis, the nodal reactive power flow equation is formulated, as shown in Equation (8):

$$Q_i = U_i \sum_{j=1}^n U_j (G_{ij} \sin \theta_{ij} - B_{ij} \cos \theta_{ij}) \quad (8)$$

Following the approach used for the active power flow equation, both sides of Equation (8) are differentiated with respect to time t , resulting in Equation (9):

$$\begin{aligned} dq_i &= \sum_{j=1}^n \frac{\partial q_i}{\partial \theta_{ij}} d\theta_{ij} + \sum_{j=1}^n \frac{\partial q_i}{\partial u_j} du_j \\ &= dq'_i + dq''_i \end{aligned} \quad (9)$$

where dq'_i represents the rate of variation of reactive power with respect to the voltage phase angle, and dq''_i denotes the rate of variation of reactive power with respect to the voltage magnitude.

dq_i'' is represents the portion with the highest rate of reactive power variation during the regulation of bus i . dq_i' provides voltage control that can be considered negligible. Using the complex frequency formula [19], dq_i'' is shown in Equation (10):

$$dq_i'' = B \cdot \zeta \tag{10}$$

where B is the imaginary component of the power grid’s admittance matrix. ζ is defined as the voltage magnitude represented by a function whose derivative is equal to the function. There is no dimension in itself. The $i - th$ component of ζ is shown in Equation (11):

$$\zeta_i \equiv \frac{dv_i}{dt} / v_i \tag{11}$$

Furthermore, B_i can be derived as the summation of the node self-conductance, the node mutual conductance, and the conductance associated with the power device.

$$dq_i \approx dq_i'' \approx B_i \cdot \zeta_i + \sum_{j=1}^n B_{i,j} \cdot \zeta_j \tag{12}$$

And B_i can be expressed as Equation (12):

$$B_i = B_{S,i} + B_{i,i} + \sum_{j=1}^n B_{i,j} \tag{13}$$

where $B_{S,i}$ represents the equivalent internal admittance of the subnets, while $B_{i,i}$ is the shunt admittance at node i .

By combining Equation (12) and Equation (13) and taking the inverse of their derivatives, the variables $x_{S,i}$ in Equation (7) can be determined.

$$B_{S,i} = \frac{dq_i'' - \sum_{j=1}^n B_{i,j} \cdot \zeta_j}{\zeta_i} - \sum_{j=1}^n B_{i,j} \tag{14}$$

So, its equivalent reactance $x_{S,i}$ can be represented by the reciprocal:

$$x_{S,i} = \frac{\zeta_i}{dq_i'' - \sum_{j=1}^n B_{i,j} \cdot \zeta_j - \zeta_i \cdot \sum_{j=1}^n B_{i,j}} \tag{15}$$

In summary, the $H_{S,i}$ can be obtained by Equations (5)–(7), and Equation (15).

$$\left\{ \begin{array}{l} dp_i = \sum_{j=1}^n \frac{\partial p_i}{\partial \theta_{ij}} d\theta_{ij} + \sum_{j=1}^n \frac{\partial p_i}{\partial u_j} du_j \\ 2H_{S,i} = \frac{dp_i}{dt} / \frac{d^2 f_{S,i}}{dt^2} \\ f_{S,i} = \Delta f_i - x_{S,i} \sum_{j=1}^n \frac{\partial p_i}{\partial \theta_{ij}} \frac{d\theta_{ij}}{dt} \\ x_{S,i} = \frac{\zeta_i}{dq_i'' - \sum_{j=1}^n B_{i,j} \cdot \zeta_j - \zeta_i \cdot \sum_{j=1}^n B_{i,j}} \end{array} \right. \tag{16}$$

In summary, Section 2 introduces the approach for evaluating the inertia time of power source nodes within a power system, with optimizations to enhance compatibility with PMU devices for data acquisition. Furthermore, the solution approach has been refined to mitigate potential singularity issues during computation.

3. Case Study

The WSCC 9-node system is utilized for simulation verification to validate the effectiveness of the power node inertia evaluation method proposed in this study. First, to confirm the accuracy of the node inertia definition equation presented herein and to eliminate potential harmonic issues arising from the randomness of new energy generation outputs and the high penetration of power electronic devices, the WSCC 9-node system is initially simulated without incorporating new energy generation equipment. Subsequently, the system is modified to include new energy generation equipment and a specified load at node 6. The inputs of these new energy generators are then varied according to a predefined profile to emulate realistic operational conditions over a typical day, enabling verification of the method's applicability to diverse power equipment. Although the random fluctuations in new energy outputs and harmonic effects of power electronic devices introduce some variability, the results consistently capture the inertia trends of the power nodes.

3.1. Case Description

In this paper, the approach is evaluated by simulations based on the WSCC 9-node system and its improved iteration. Figure 3 illustrates the conventional WSCC 9-node system [20], where the synchronous generator module adopts the model provided in the Simulink library. This model incorporates a specified inertia time constant. The key parameters of the synchronous generator set are summarized in Table 1. The generator connected to node 2 is selected for detailed analysis to validate the accuracy of the proposed method. PMU devices are installed at node 2 and their connected node 7 to capture critical data, including nodal voltage magnitude, voltage phase angle, and frequency, which are essential for the calculation process.

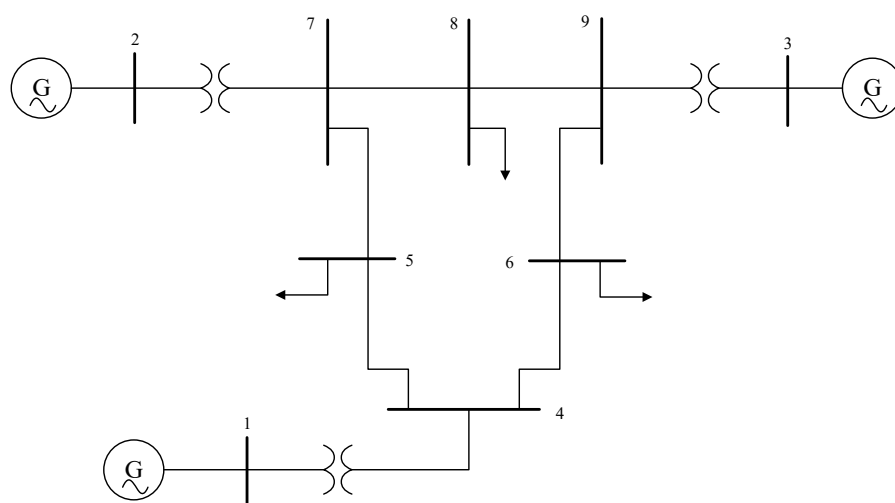


Figure 3. The topological structure of the power system network of WSCC9.

Table 1. Detailed data of synchronous generators.

Number	P_N (MW)	H (s)
1	247.3	23.6
2	192	6.4
3	128	3.01

3.2. Results

Simulation tests were conducted on a system composed entirely of synchronized power equipment to validate the accuracy of the approach for estimating the equivalent inertial time constants of power nodes. At $t = 40$ s, a sudden active power disturbance was introduced under two scenarios: Scenario 1, involving a sudden 5% decrease in load,

and Scenario 2, involving a sudden 5% increase in load. These scenarios were designed to assess the method’s accuracy for both positive and negative active power deficits. The simulation results are presented in Figure 4.

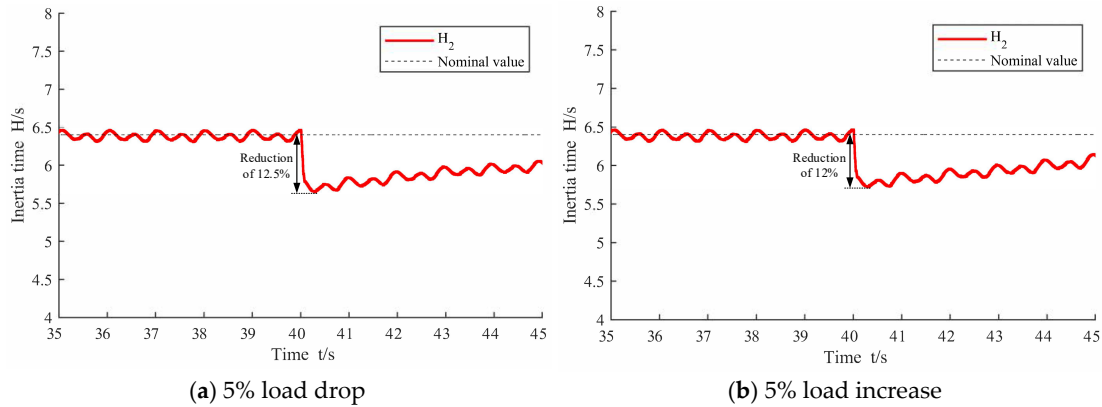


Figure 4. Estimated value waveform during a 5% load flow.

Following the verification of the accuracy of the synchronous generator model, the traditional WSCC 9-node system is enhanced by integrating a wind power plant and two photovoltaic power plants with associated loads at node 6. In this simulation, the inertia time constants are estimated for various nodes: the synchronous generator at node 2, the virtual power plant at node 6, the wind power plant at node D5, and the two PV power plants at nodes D2 and D7. The proportion of renewable energy is varied by adjusting the number and output power of new energy plants connected to the system to investigate the impact of renewable energy penetration. Additionally, stochasticity in the output power of these plants is simulated by assigning varying input profiles to the new energy generators, reflecting real operating conditions. The enhanced WSCC 9-node topology is depicted in Figure 5, while the input profiles of the new energy plants are illustrated in Figure 6. The rated capacities and virtual inertia time constants of the connected renewable energy plants are summarized in Table 2.

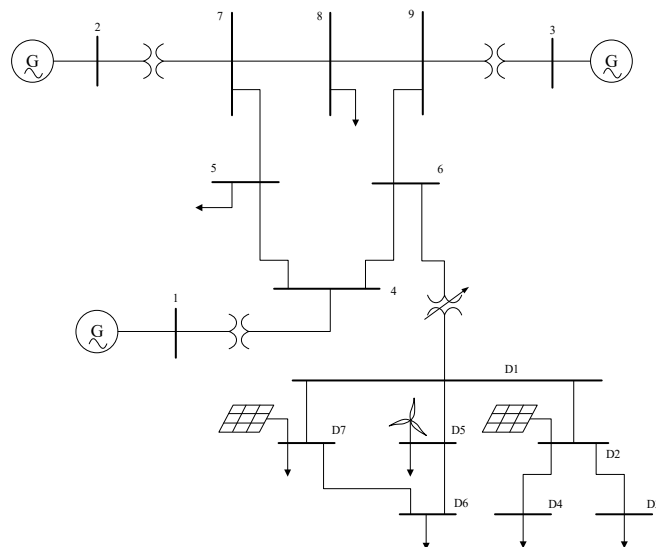


Figure 5. Topology of the WSCC9 power system network after adding renewable energy sources.

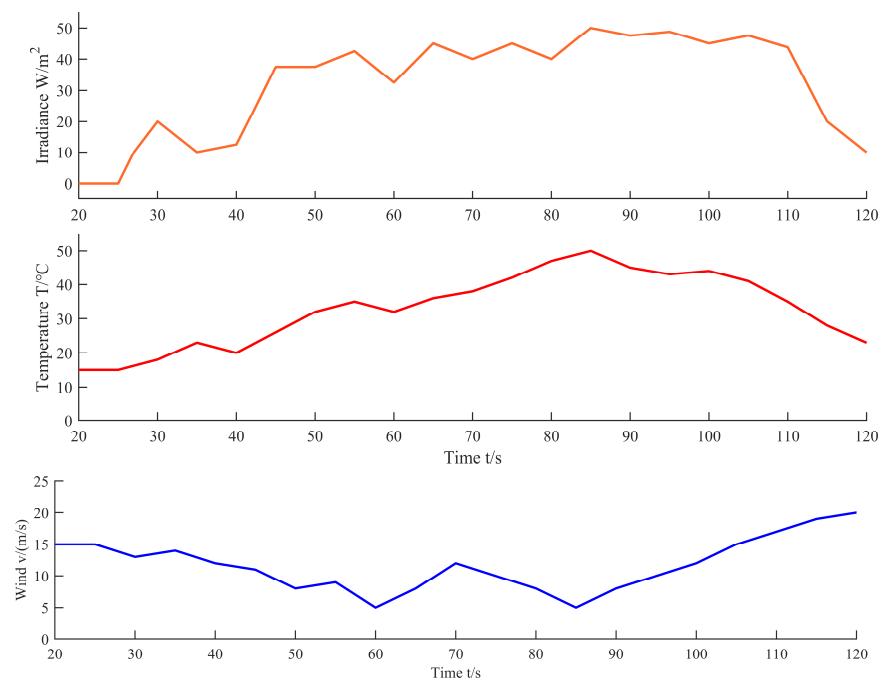


Figure 6. The input value for the renewable energy unit.

Table 2. Detailed data on renewable energy equipment.

Number	P_N (MW)	H_V (s)
D2	30	2~4
D5	60	2~4
D7	50	2~4

The renewable energy penetration of the system is regulated by adjusting the number of connected renewable energy plants and their output power to achieve penetration levels of 5%, 10%, and 15%, respectively. The estimated inertia time H_2 for generator G2 connected to node 2 under these three scenarios is illustrated in Figure 7, with the corresponding detailed data presented in Table 3.

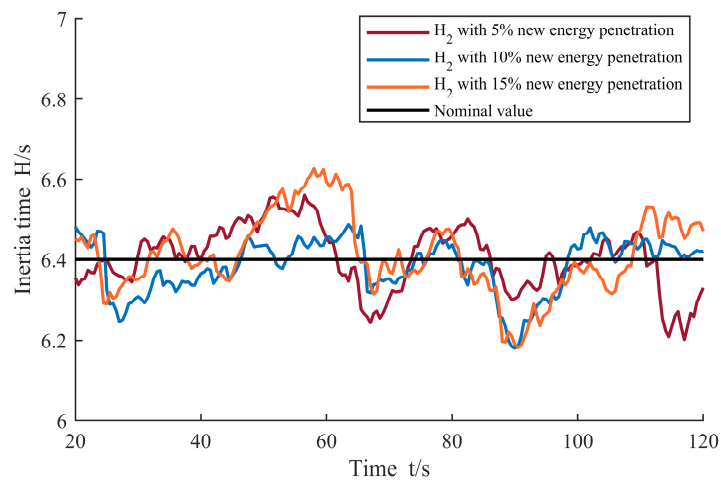
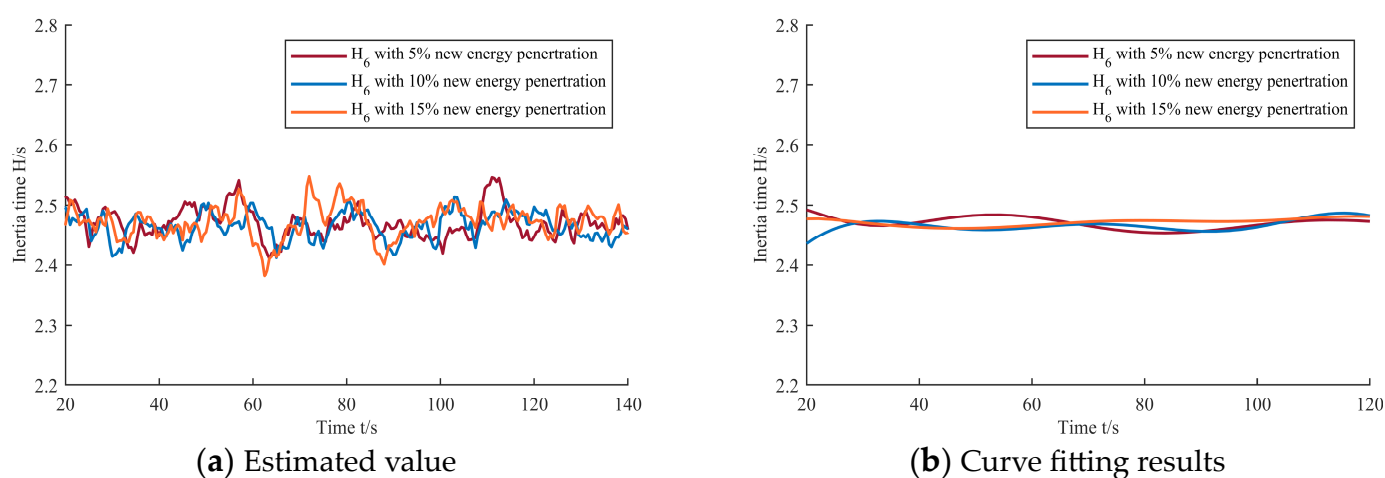


Figure 7. H_2 at different new energy penetration rates.

Table 3. Detailed data.

Renewable Energy Penetration	Minimum	Maximum	Average
5%	6.202	6.560	6.406
15%	6.180	6.495	6.393
25%	6.175	6.626	6.381

This study evaluates the inertia time H_6 at node 6 to validate further the feasibility of the proposed method for estimating inertia time at the virtual power plant access node. Given that the stochastic output of renewable energy power plants and the harmonics generated by power electronic devices can influence the estimated inertia time, curve fitting is applied to the evaluation results to mitigate these effects. Simulations are conducted under three different renewable energy penetration levels, with the specific results illustrated in Figure 8, and the key data summarized in Table 4.

**Figure 8.** H_6 at different new energy penetration rates.**Table 4.** Detailed data.

Renewable Energy Penetration	Minimum	Maximum	Average
5%	2.410	2.544	2.465
15%	2.407	2.545	2.466
25%	2.380	2.546	2.467

The inertia time of the renewable energy devices used in this simulation ranges from 2 to 4 s, aligning closely with the evaluation results and demonstrating the feasibility of the proposed method [21]. As the penetration increases, the greater variability in the output of renewable energy plants and the harmonic effects of power electronic devices influence the estimation results. Nonetheless, this variability contributes to a slight overall increase in the total inertia time.

Finally, this study estimates the node inertia time for three different renewable energy plant access nodes—D2, D5, and D7—under a renewable energy penetration level of 15%. The corresponding estimates are presented in Figure 9.

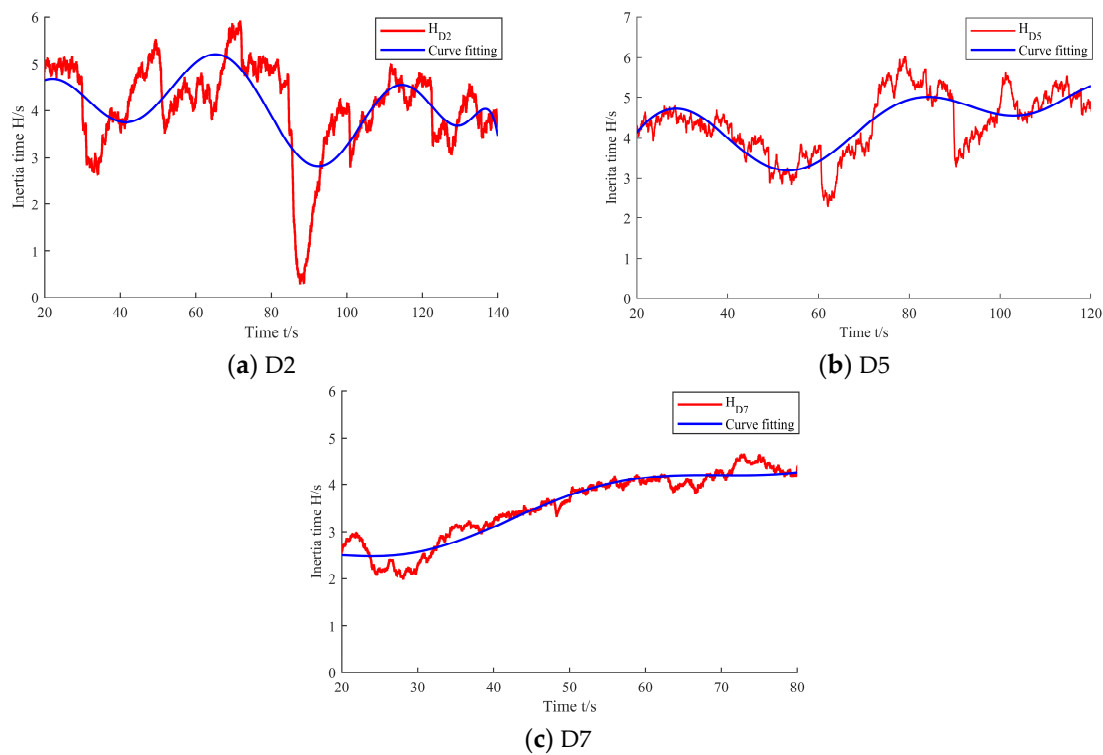


Figure 9. The node inertia time for different renewable energy plant access nodes —D2, D5, and D7.

3.3. Discussion

In Sections 3.1 and 3.2, the method outlined in Section 2 is validated through simulations, with further discussion of the results provided in Section 3.3. A summary of key data from the various scenarios in Section 3.2 is presented in Table 5.

Table 5. The average inertia time constant evaluation value in Section 3.2.

Renewable Energy Penetration	H_2	Deviation	H_6
0%	6.402	0.03%	-
5%	6.406	0.09%	2.465
15%	6.393	1.09%	2.466
25%	6.381	2.97%	2.467

As shown in Table 5, for nodes exclusively connected to synchronous generation equipment, the proposed methodology demonstrates a high level of accuracy in assessing equivalent inertial time constants, with deviations of less than 3%, even under disturbances from renewable energy sources. In contrast, nodes connected to non-synchronous generating equipment exhibit greater fluctuations in the evaluation results, although the average values remain consistently accurate.

A simulation study of the conventional WSCC 9-node system was conducted to analyze the online estimation of the equivalent inertia time H_2 for generator G2 connected to node 2 during an active power deficit. The variation curve is presented in Figure 2. Upon comparing the results, it was observed that the equivalent inertia time of node 2 decreases consistently, regardless of whether the active power deficit is positive or negative, with a similar reduction of approximately 12%. This finding indicates that during power disturbances, the rotational inertia of synchronous generator G2 actively responds to resist the frequency change, a process corresponding to the inertia phase. As a result, the generator sacrifices its inertia, reducing the estimated inertia time. Once the subsequent frequency regulation system is activated, the influence of inertia on frequency diminishes,

and the estimated inertia time gradually returns to its nominal value. Comparing the estimated inertia time for node 2 with the rated inertia time constant of synchronous generator G2 (6.4 s), the estimated values exhibit stable fluctuations around the rated value prior to disturbances. Following an active power deficit, the estimated inertia time decreases as expected, aligning with theoretical predictions. These results validate the scientific soundness of the node inertia time definition and confirm the accuracy of the proposed estimation method.

A comparison of Figures 6 and 9 reveals a correlation between the inertia time fluctuation characteristics and the output power of the new energy power plants. Specifically, the estimated inertia time tends to be higher when the output power of the new energy plants is greater and lower when the output power is reduced. Additionally, due to the proximity of the inverter at the outlet, the inertia time estimation is more significantly affected by harmonics. Since the proposed node inertia time estimation method involves differentiation, the impact of harmonics on the results is further amplified. From Figure 9 and Table 2, it can be observed that while the randomness of the new energy output and the harmonic effects of power electronic equipment influence the estimation results, the estimated inertia time of the corresponding nodes aligns closely with the set value of 2–4 s after curve fitting. For node 6 in the improved WSCC 9-node system, the estimated inertia time is relatively lower. This reduction is attributable to the fact that the connected virtual power plant carries a certain load and is located at a distance from the plant. Consequently, the estimated inertia time for node 6 is approximately 2.4 s, which is consistent with expectations.

4. Conclusions

This paper proposes an online method for estimating the equivalent inertia time constant of power generation equipment based on the nodal power flow equation. By leveraging real-time data from PMUs and the power system's nodal power flow equations, the method simplifies online inertia estimation. Instead of emphasizing the dynamic characteristics of power equipment operation, it focuses on the power injected into the nodes. Crucially, this approach delivers accurate estimates of inertia time constants for a wide range of power devices, effectively addressing the variability and uncertainty inherent to renewable energy sources and their fluctuating outputs. The method enables real-time estimation of the system's overall inertia level by deploying PMU devices solely at power plant access nodes and their associated nodes, significantly reducing the required number of PMU installations and lowering operational costs. Simulation results confirm the feasibility of the methodology for synchronous generators, while additional validation demonstrates its applicability to diverse types of power-generating equipment, underscoring its broad versatility. This approach offers a more precise framework for assessing and managing system inertia, thereby contributing to the stable and reliable operation of power systems.

Author Contributions: Conceptualization, Z.Z.; methodology, X.W.; software, Y.S.; validation, Z.Z.; investigation, X.W.; resources, X.W.; data curation, X.W.; writing—original draft preparation, X.W.; writing—review and editing, Z.Z.; visualization, J.S.; supervision, Z.Z.; project administration, Y.W.; funding acquisition, Q.Z. All authors have read and agreed to the published version of the manuscript.

Funding: This research was funded by Zhenjiang Key R&D Plan (Industry Foresight and Common Key Technology) grant number GY2023001.

Data Availability Statement: The original contributions presented in this study are included in the article. Further inquiries can be directed to the corresponding author(s).

Acknowledgments: This work was fully funded by Zhenjiang Key R&D Plan (Industry Foresight and Common Key Technology), Project Award Number: GY2023001.

Conflicts of Interest: The authors declare that they have no conflicts of interest to report regarding the present study.

References

1. Farmer, W.J.; Rix, A.J. Evaluating power system network inertia using spectral clustering to define local area stability. *Int. J. Electr. Power Energy Syst.* **2022**, *134*, 107404. [[CrossRef](#)]
2. Johnson, S.C.; Papageorgiou, D.J.; Mallapragada, D.S.; Deetjen, T.A.; Rhodes, J.D.; Webber, M.E. Evaluating rotational inertia as a component of grid reliability with high penetrations of variable renewable energy. *Energy* **2019**, *180*, 258–271. [[CrossRef](#)]
3. Jiang, C.; Cai, G.; Yang, D.; Liu, X.; Hao, S.; Li, B. Multi-objective configuration and evaluation of dynamic virtual inertia from DFIG based wind farm for frequency regulation. *Int. J. Electr. Power Energy Syst.* **2024**, *158*, 109956. [[CrossRef](#)]
4. Zhang, G.; Ren, J.; Zeng, Y.; Liu, F.; Wang, S.; Jia, H. Security assessment method for inertia and frequency stability of high proportional renewable energy system. *Int. J. Electr. Power Energy Syst.* **2023**, *153*, 109309. [[CrossRef](#)]
5. Dimoulias, S.C.; Kontis, E.O.; Papagiannis, G.K. On-line tracking of inertia constants using ambient measurements. *Electr. Power Syst. Res.* **2023**, *224*, 109643. [[CrossRef](#)]
6. Hu, P.; Li, Y.; Yu, Y.; Blaabjerg, F. Inertia estimation of renewable-energy-dominated power system. *Renew. Sustain. Energy Rev.* **2023**, *183*, 113481. [[CrossRef](#)]
7. Zhang, H.; Yu, S.; Zhang, X.; Gao, Z. Fast power correction based transient frequency response strategy for energy storage system in low-inertia power systems. *J. Energy Storage* **2024**, *97*, 112955. [[CrossRef](#)]
8. Biyya, I.; Oubrahim, Z.; Abbou, A. Frequency and ROCOF estimation under steady-state and dynamic conditions for three-phase grid-connected converters. *Electr. Power Syst. Res.* **2023**, *224*, 109723. [[CrossRef](#)]
9. Lugnani, L.; Dotta, D.; Lackner, C.; Chow, J. ARMAX-based method for inertial constant estimation of generation units using synchrophasors. *Electr. Power Syst. Res.* **2020**, *180*, 106097. [[CrossRef](#)]
10. Bizzarri, F.; Giudice, D.d.; Grillo, S.; Linaro, D.; Brambilla, A.; Milano, F. Inertia Estimation Through Covariance Matrix. *IEEE Trans. Power Syst.* **2024**, *39*, 947–956. [[CrossRef](#)]
11. Skopetou, N.E.; Sfetkos, A.I.; Kontis, E.O.; Papadopoulos, T.A.; Chrysochos, A.I. Identification of inertia constants using time-domain vector fitting. *Electr. Power Syst. Res.* **2024**, *236*, 110924. [[CrossRef](#)]
12. Wang, Q.; Yao, L.; Xu, J.; Cheng, F.; Mao, B.; Wen, Z.; R., C. S-MCMC Based Equivalent Inertia Probability Evaluation for Power Systems With High Proportional Renewable Energy. *Power Syst. Technol.* **2024**, *48*, 140–149.
13. Ma, J.; Su, Y.; Wang, C.; Peng, Y.; Shi, L.; Yu, Y. Inertia identification of power system based on energy function method. *Energy Rep.* **2024**, *11*, 2893–2900. [[CrossRef](#)]
14. Zhao, Y.; Liu, T.; Hill, D.J. Data-driven adaptive predictive frequency control for power systems with unknown and time-varying inertia. *Electr. Power Syst. Res.* **2024**, *234*, 110815. [[CrossRef](#)]
15. Zhang, Z.; Preece, R. Effects of inertia distribution on regional frequency heterogeneity. *Electr. Power Syst. Res.* **2024**, *231*, 110340. [[CrossRef](#)]
16. Shan, Y.; Wang, Z.; Wu, J.; Gao, H. Evaluation of the inertia distribution performance for multi-machine power system. *Int. J. Electr. Power Energy Syst.* **2024**, *155*, 109595. [[CrossRef](#)]
17. Sfetkos, A.I.; Kontis, E.O.; Papadopoulos, T.A.; Papagiannis, G.K. Inertia estimation of multi-area power systems using tie-line measurements and modal sensitivity analysis. *Electr. Power Syst. Res.* **2023**, *224*, 109642. [[CrossRef](#)]
18. Milano, F.; Ortega, Á. A Method for Evaluating Frequency Regulation in an Electrical Grid—Part I: Theory. *IEEE Trans. Power Syst.* **2021**, *36*, 183–193. [[CrossRef](#)]
19. Milano, F. Complex Frequency. *IEEE Trans. Power Syst.* **2022**, *37*, 1230–1240. [[CrossRef](#)]
20. Bernal, R.; Milano, F. Improving voltage and frequency control of DERs through Dynamic Power Compensation. *Electr. Power Syst. Res.* **2024**, *235*, 110768. [[CrossRef](#)]
21. Tan, B.; Zhao, J.; Netto, M.; Krishnan, V.; Terzija, V.; Zhang, Y. Power system inertia estimation: Review of methods and the impacts of converter-interfaced generations. *Int. J. Electr. Power Energy Syst.* **2022**, *134*, 107362. [[CrossRef](#)]

Disclaimer/Publisher’s Note: The statements, opinions and data contained in all publications are solely those of the individual author(s) and contributor(s) and not of MDPI and/or the editor(s). MDPI and/or the editor(s) disclaim responsibility for any injury to people or property resulting from any ideas, methods, instructions or products referred to in the content.